View metadata, citation and similar papers at core.ac.uk
brought to you by CORE
provided by Flinders Academic Commons

AMERICAN ACADEMY OF OPHTHALMOLOGY®

Biallelic *CPAMD8* Variants Are a Frequent Cause of Childhood and Juvenile Open-Angle Glaucoma

Owen M. Siggs, MD, DPhil,[1] Emmanuelle Souzeau, PhD,[1] Deepa A. Taranath, FRANZCO,[1] Andrew Dubowsky, PhD,[2] Angela Chappell, BAppSci,[1] Tiger Zhou, BMBS,[1] Shari Javadiyan, PhD,[1] Jillian Nicholl, PhD,[2] Lisa S. Kearns, BOrth&OphthalSci,[3] Sandra E. Staffieri, PhD,[3,4,5] Andrew Narita, FRANZCO,[6] James E.H. Smith, FRANZCO,[7,8,9] John Pater, FRANZCO,[1] Alex W. Hewitt, FRANZCO, PhD,[3,4,10] Jonathan B. Ruddle, FRANZCO,[4,5] James E. Elder, FRANZCO,[4,11] David A. Mackey, FRANZCO, MD,[10,12] Kathryn P. Burdon, PhD,[1,10] Jamie E. Craig, FRANZCO, DPhil[1]

Purpose: Developmental abnormalities of the ocular anterior segment in some cases can lead to ocular hypertension and glaucoma. *CPAMD8* is a gene of unknown function recently associated with ocular anterior segment dysgenesis, myopia, and ectopia lentis. We sought to assess the contribution of biallelic *CPAMD8* variants to childhood and juvenile open-angle glaucoma.

Design: Retrospective, multicenter case series.

Participants: A total of 268 probands and their relatives with a diagnosis of childhood or juvenile open-angle glaucoma.

Purpose: Developmental abnormalities of the ocular anterior segment in some cases can lead to ocular hypertension and glaucoma. *CPAMD8* is a gene of unknown function recently associated with ocular anterior segment dysgenesis, myopia, and ectopia lentis. We sought to assess the contribution of biallelic *CPAMD8* variants to childhood and juvenile open-angle glaucoma.

Methods: Patients underwent a comprehensive ophthalmic assessment, with DNA from patients and their relatives subjected to genome, exome, or capillary sequencing. *CPAMD8* RNA expression analysis was performed on tissues dissected from cadaveric human eyes.

Main Outcome Measures: Diagnostic yield within a cohort of childhood and juvenile open-angle glaucoma, prevalence and risk of ophthalmic phenotypes, and relative expression of *CPAMD8* in the human eye.

Results: We identified rare (allele frequency $< 4\times10^{-5}$) biallelic *CPAMD8* variants in 5.7% (5/88) of probands with childhood glaucoma and 2.1% (2/96) of probands with juvenile open-angle glaucoma. When including family members, we identified 11 individuals with biallelic variants in *CPAMD8* from 7 unrelated families. Nine of these individuals were diagnosed with glaucoma (9/11, 81.8%), with a mean age at diagnosis of 9.22±14.89 years, and all individuals with glaucoma required 1 or more incisional procedures to control high intraocular pressure. Iris abnormalities were observed in 9 of 11 individuals, cataract was observed in 8 of 11 individuals (72.7%), and retinal detachment was observed in 3 of 11 individuals (27.3%). *CPAMD8* expression was highest in neural crest–derived tissues of the adult anterior segment, suggesting that *CPAMD8* variation may cause malformation or obstruction of key drainage structures.

Conclusions: Biallelic *CPAMD8* variation was associated with a highly heterogeneous phenotype and in our cohorts was the second most common inherited cause of childhood glaucoma after *CYP1B1* and juvenile open-angle glaucoma after *MYOC*. *CPAMD8* sequencing should be considered in the investigation of both childhood and juvenile open-angle glaucoma, particularly when associated with iris abnormalities, cataract, or retinal detachment. *Ophthalmology 2020;■:1–9 © 2020 by the American Academy of Ophthalmology. This is an open access article under the CC BY-NC-ND license (http://creativecommons.org/licenses/by-nc-nd/4.0/).*

Supplemental material available at www.aaojournal.org.

Anterior segment dysgenesis (ASD) is a heterogeneous group of ocular developmental disorders affecting the iris, cornea, lens, or aqueous humor outflow structures and is frequently associated with secondary glaucoma. Associated defects include hypoplasia of the iris stroma, corectopia, pseudopolycoria, posterior embryotoxon, abnormal iridocorneal angle, iridocorneal adhesions, corneal opacity, and corneal vascularization. The most common ASD

© 2020 by the American Academy of Ophthalmology
This is an open access article under the CC BY-NC-ND license (http://creativecommons.org/licenses/by-nc-nd/4.0/). Published by Elsevier Inc.

https://doi.org/10.1016/j.ophtha.2019.12.024
ISSN 0161-6420/20

presentation is Axenfeld-Rieger anomaly, known as "Axenfeld-Rieger syndrome" (ARS), when associated with systemic features. Individuals with ARS have a 50% to 60% lifetime risk of developing glaucoma, which can occur as early as the first year of life.[1,2]

Discriminating between primary and secondary glaucoma can be particularly challenging in childhood because of their occasional phenotypic overlap, the lack of certain abnormalities at birth, and the difficulty of a thorough eye examination in infants and young children.[3,4] For example, although heterozygous variants in *FOXC1*[5] or *PITX2*[6] account for 40% to 60% of ARS, *FOXC1* variants may also be associated with childhood glaucoma with only mild features of ASD.[4] This diagnostic challenge is further highlighted by the occasional misdiagnosis of other congenital conditions as childhood glaucoma, including X-linked megalocornea or congenital hereditary endothelial dystrophy.[7]

Recently, a unique form of autosomal recessive ASD was associated with variants in *CPAMD8* (ASD 8, Online Mendelian Inheritance in Man 617319).[8] Unlike other ASD cases, none of the 4 original cases with biallelic *CPAMD8* variants had glaucoma; only a single case was reported to have developed ocular hypertension at 49 years of age, suspected to have been exacerbated by ectopia lentis and retinal surgery.[8] Subsequently, congenital glaucoma associated with lens subluxation was reported in a single case with a homozygous frameshift variant in *CPAMD8*, although no other clinical details were provided.[3] A homozygous variant in *CPAMD8* has also been associated with Morgagnian cataract in Red Holstein Friesian cattle, with glaucoma observed in 1 of 8 eyes examined and associated with uveitis and retinitis in the same eye.[9]

We investigated *CPAMD8* variation in a cohort of patients with childhood glaucoma or juvenile open-angle glaucoma diagnosed between 18 and 40 years of age. Compound heterozygous or homozygous *CPAMD8* variants were identified in 11 affected individuals from 7 families, each with a unique combination of anterior segment abnormalities and secondary glaucoma.

Methods

Patient Recruitment

Patients and family members were recruited via the Australian & New Zealand Registry of Advanced Glaucoma[10] and provided written informed consent under protocols approved by the Southern Adelaide Clinical Human Research Ethics Committee. The study was conducted in accordance with the revised Declaration of Helsinki and followed the National Health and Medical Research Council statement of ethical conduct in research involving humans. Clinical diagnosis and details were obtained from the treating ophthalmologist, and consent to publish photographs was obtained from individuals or their legal guardians. Parents and siblings of affected individuals were recruited when available. Childhood glaucoma was defined as an onset of glaucoma before 18 years of age as per The Childhood Glaucoma Research Network classification system: in this cohort, cases had been referred with a suspected diagnosis of primary congenital glaucoma, which in some patients was later revised.[11] The juvenile open-angle glaucoma cohort consisted of individuals diagnosed between 18 and 40 years of age. All childhood and juvenile open-angle glaucoma cases were screened for biallelic *CYP1B1* variants by capillary sequencing, with all juvenile open-angle glaucoma cases also screened for heterozygous *MYOC* variants. Each cohort included both advanced and nonadvanced glaucoma cases.

DNA Sequencing and Analysis

DNA was prepared from whole blood or saliva samples. Genomes were sequenced on the Illumina Hiseq X platform as previously described.[12] Exome capture was performed using the Agilent SureSelect system (v4 or v5) and sequenced on an Illumina HiSeq (2000 or 2500).[13] Raw reads were aligned to the hg19 reference using BWA-MEM (v0.7.12) and sorted and duplicate-marked with Picard (v1.13). Local indel realignment and base quality score recalibration were performed using GATK (v3.4.0). Variants were recalibrated using GATK Variant Quality Score Recalibrator. The VCF files were annotated with ANNOVAR using RefSeq, gnomAD (r2.0.2), 1000 Genomes (Phase 3), NHLBI-ESP project (v2), ClinVar (20170905), and dbNSFP (v3.3a) databases. The Combined Annotation Dependent Depletion (CADD), Sorting Intolerant From Tolerant, and PolyPhen-2 HumVar tools were used to predict the effect of coding sequence variants on protein function. Protein sequences were aligned with Clustal Omega and BOXSHADE.

For initial variant filtering, we considered the subset of nonsense, essential splice, missense, or frameshift PASS variants with a gnomAD allele frequency < 0.001, genotype quality score of > 20, and allele balance of > 0.25. With the exception of essential splice variants, noncoding variants were not considered. All 7 probands with biallelic variants in *CPAMD8* had no rare variants (at an allele frequency threshold of 0.0001) in *CYP1B1*, *MYOC*, *FOXC1*, or *PITX2*. Variants identified through genome and exome sequencing were confirmed in a National Association of Testing Authorities—accredited laboratory (SA Pathology, Flinders Medical Centre, Adelaide, Australia) using bidirectional capillary sequencing of the relevant polymerase chain reaction—amplified *CPAMD8* region. Primer sequences are available upon request. Polymerase chain reaction products were sequenced, and base called on the Applied Biosystems 3130*xl* Genetic Analyzer (Thermo Fisher Scientific, Waltham, MA). Detection of sequence variants was performed with the aid of Mutation Surveyor v4.0 (SoftGenetics LLC, State College, PA), with trace files assembled against the *CPAMD8* (NM_015692.2) hg19 reference. Variants have been submitted to ClinVar (https://www.ncbi.nlm.nih.gov/clinvar/).

Clinical Single Nucleotide Polymorphism Array

A masked array of *CPAMD8* copy number variation (GRCh37 assembly, 19:17003758-17137625) was performed using the Illumina Infinium CytoSNP-850k Beadchip. Copy number variants were called if 10 or more consecutive single nucleotide polymorphisms were suggestive of copy number gain or loss, giving an average effective resolution of <0.1 Mb.

Tissue Dissection and RNA Preparation

Cadaveric human eyes with no known ocular disease and otherwise unsuitable for corneal transplantation were obtained from the Eye Bank of South Australia. Tissue dissection was performed under light microscope with a mean postmortem time of 9.7±5.3 hours. Tissues from the corneal epithelium, corneal stroma, corneal endothelium, trabecular meshwork, pars plicata of the ciliary body, retina, optic nerve head, and optic nerve were collected and fixed in

RNAlater solution for approximately 5 days before storage at −80°C. A standard Trizol extraction protocol was used for RNA isolation. RNA extracted from the pars plicata was passed through a Genomic-tip 20/G (Qiagen, Hilden, Germany) as per the manufacturer's instructions to remove excess melanin. RNA quality was assessed using the Agilent (Santa Clara, CA) Bioanalyzer 2100 RNA 6000 Nano Assay (mean RIN = 6.5±1.8). A Qubit 2.0 Fluorometer (Thermo Fisher Scientific) was used to quantify RNA.

RNA Sequencing and Analysis

RNA libraries were prepared using the Bioo Scientific (Austin, TX) NEXTflex Rapid Directional RNA-Seq Kit Bundle with RNA-Seq Barcodes and poly(A) beads (NOVA-5138-10). Total RNA from each tissue sample (250 ng) was prepared for individual sequencing. Sequencing was performed on an Illumina NextSeq 500 using High Output v2 Kit (75 cycles) after sample enrichment with 16 cycles of polymerase chain reaction. Phi X DNA was spiked into each run pool. Trimgalore v0.4.0 was used to trim sequence adaptors and low-quality bases (Phred scores < 28). Remaining reads were aligned to the human genome (GRCh38 assembly) using TopHat v2.1.1, allowing for 2 mismatches per read and no ambiguous reads. Uniquely aligned reads were annotated using the union model in HTSeq-count v0.6.0 with Ensembl version 84 human gene ID. Trimmed mean of M-values was used to normalize count data, followed by calculation of differential expression in EdgeR v3.10.2. Benjamini−Hochberg adjustment was applied for false discovery rate correction.

Results

To investigate an underlying genetic architecture of childhood glaucoma, we recruited a cohort of 129 probands with a diagnosis of childhood glaucoma. All 129 probands were prescreened for biallelic variants in *CYP1B1*, which accounted for 21 cases (16.3%). For the remaining 108 probands, we sequenced and analyzed 87 exomes and 1 genome for variants in *CPAMD8*. We identified rare (gnomAD allele frequency < 0.001) compound heterozygous missense, nonsense, and frameshift variants in 7 individuals from 5 unrelated families (Fig 1A−D), consistent with suspected autosomal recessive inheritance in all families. In a cohort of 206 ancestrally matched controls without glaucoma, only 1 individual carried more than 1 rare *CPAMD8* coding variant (both missense, phase unknown), with neither variant predicted to be damaging (Phred-scaled CADD score of < 6). In family 1, the affected proband (II:1), but not his unaffected sister (II:2), was a compound heterozygote for variants inherited from either parent. In family 2, the proband (II:1) was conceived via sperm donation, with the unaffected mother and unaffected father each confirmed to carry separate heterozygous variants. In family 3, 2 affected sisters (II:1 and II:3), but not a third unaffected sister (II:2), carried the same pair of compound heterozygous variants, with 1 variant carried by each unaffected parent (Fig 1A).

Two probands (families 4 and 5) were heterozygous for the previously described c.2352dupC frameshift insertion variant of *CPAMD8* (p.(Arg785GlnfsTer23)).[8] Both probands had ocular features consistent with *CPAMD8*-associated ASD (Fig 2), including iris stromal hypoplasia, phacodonesis, iridodonesis, ectropion uveae, elevated intraocular pressure (IOP), and glaucoma, yet neither proband had a nonsense, essential splice, frameshift, or missense variant on the second *CPAMD8* allele to explain the expected autosomal recessive inheritance pattern. To broaden our search for a second disease-associated *CPAMD8* variant in these families, we evaluated larger copy-number variants that are more readily detected by genome sequencing or single nucleotide polymorphism array than by capture-based short-read exome sequencing. By using single nucleotide polymorphism array analysis, we identified a maternally inherited 16 Kb heterozygous duplication (chr19:g.17099980_17116595) in family 4, spanning exons 8 to 13 of *CPAMD8*. Genome sequencing was performed to characterize the nature of the duplication, which revealed a direct tandem duplication of exons 8 to 13 of *CPAMD8* (Fig 1C). This was predicted to introduce a frameshift downstream of exon 8, with subsequent nonsense-mediated decay of *CPAMD8* transcript (Fig 1D).

Given the absence of larger copy number variants in family 5, we expanded our search to in-frame insertion or deletion variants. This revealed a multinucleotide variant comprising a 3 nucleotide in-frame insertion (c.3231_3232insGGA, p.(Leu1077_Ser1078insGly)), along with an adjacent synonymous single nucleotide variant. Together, these variants created a 4-nucleotide duplication of an upstream sequence (TCCC), forming part of a larger 8 nucleotide tandem repeat (TCCCAGGA**TCCC**AGGA). Although this multinucleotide variant did not alter the *CPAMD8* reading frame, it did introduce an additional glycine amino acid into the highly conserved farnesyl o-methyltransferase domain (Fig 1). Because both parents were deceased, we were unable to resolve the phase of each *CPAMD8* variant.

To test the possibility that *CPAMD8* variation contributes to glaucoma later in life, we also investigated a cohort of 139 probands diagnosed with juvenile open-angle glaucoma between 18 and 40 years of age. All cases were screened for variants in *MYOC* and *CYP1B1*, which accounted for 5 (3.6%) and 2 (1.4%) cases, respectively. Of the remaining 132 probands, we sequenced 96 exomes, which revealed an additional 2 probands with biallelic *CPAMD8* variants. After screening relatives, a total of 4 individuals with homozygous loss-of-function *CPAMD8* variants were identified within 2 consanguineous families (families 6 and 7) (Fig 1A). Two of these individuals were diagnosed with juvenile open-angle glaucoma, and 1 was receiving treatment for ocular hypertension. Two cases (family 7, II:1 and II:2) had a clinical diagnosis of Stickler syndrome, although we found no evidence of rare and predicted pathogenic variants in any of the Stickler-associated genes (*COL2A1, COL9A1, COL9A2, COL9A3, COL11A1, COL11A2*).

All 10 *CPAMD8* variants identified were rare or absent in gnomAD at a frequency consistent with a rare recessive disease (Table 1), with no observed homozygotes. Families 2 and 3 were not known to be related but both are of Scottish ancestry and shared a single variant (p.(Thr1433Asn)) found only in the non-Finnish European cohort of gnomAD (5/125954 alleles). All identified *CPAMD8* missense variants were predicted to be damaging by the CADD, PolyPhen-2, or Sorting Intolerant From

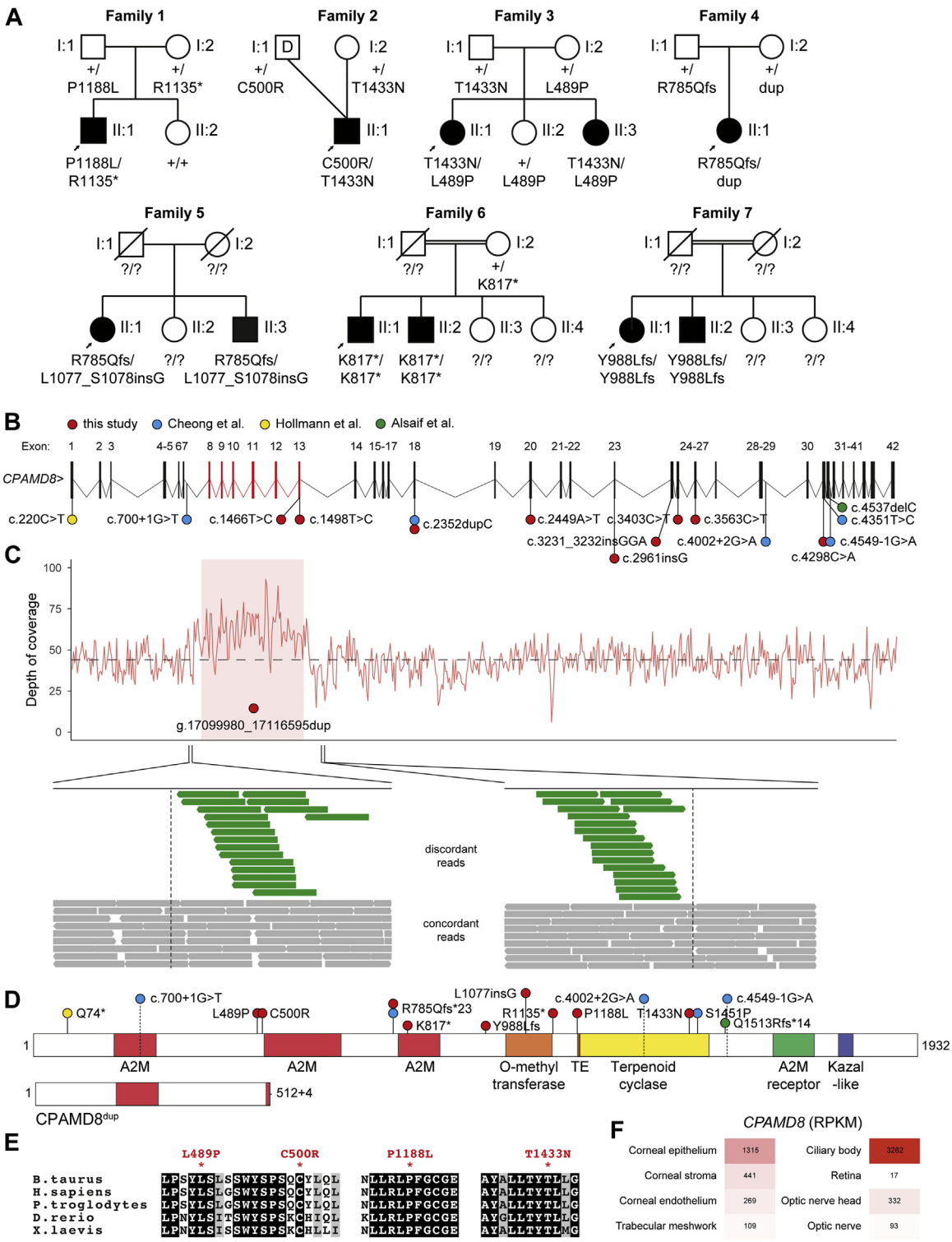

Figure 1. Childhood glaucoma with anterior segment dysgenesis (ASD) in individuals with biallelic *CPAMD8* variants. **A,** Pedigrees of the 7 families described in this study. In family 2, the proband was conceived via a sperm donor. **Round symbols** indicate female patients; **square symbols** indicate male patients; **black symbols** indicate childhood glaucoma; **arrow** indicates proband. D = sperm donor; + = reference allele. **B,** *CPAMD8* locus and location of disease-associated variants described in this study and others.[3,8,9] **C,** Direct tandem duplication encompassing *CPAMD8* exons 8–13, as identified by short-read genome sequencing. **D,** CPAMD8 protein schematic and domain structure showing the location of disease-associated missense, nonsense, and frameshift variants (location of relevant splice junctions and splice variants are indicated with **dashed lines**). A2M = α2-macroglobulin domain; TE = thioester site. **E,** CPAMD8 protein sequence alignments across multiple vertebrate species. Residues of interest are highlighted for variants p.(Leu489Pro), p.(Cys500Arg), p.(Pro1188-Leu), and p.(Thr1433Asn). **F,** *CPAMD8* expression in adult human donor ocular tissue. RPKM = reads per kilobase per million mapped reads.

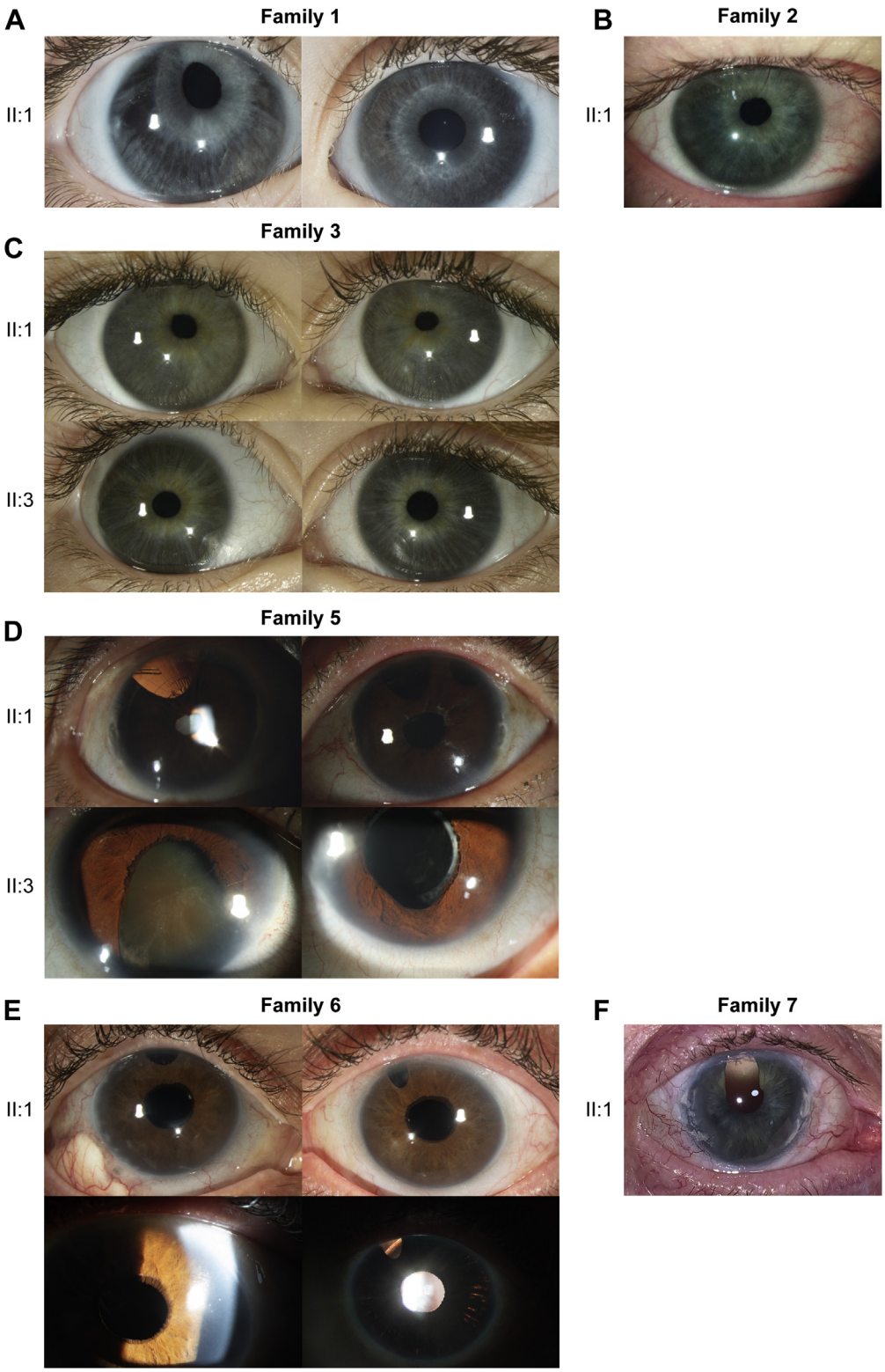

Figure 2. ASD phenotypes in individuals with biallelic *CPAMD8* variants. **A–D,** Clinical photographs of the right eye (RE, **left** panels) and the left eye (LE, **right** panels) of the specified individuals. Family 1 **(A)**: superior corectopia, initially suspected to be secondary to trabeculotomy surgery (**A**, RE) and iris stromal hypoplasia **(A,** both eyes). Family 2 (**B,** RE): subtle superonasal corectopia and mild iris stromal hypoplasia. Family 3 **(C)**: superonasal corectopia (II:1, both eyes; II:3, LE), iris stromal hypoplasia (II:3, both eyes). Family 5 **(D)**: bilateral superior iridectomies (II:1); inferior iris coloboma, dense nuclear cataract, ectropion uveae (II:3, RE); partial inferior iris coloboma, ectropion uveae (II:3, LE). Family 6 **(F)**: bilateral iridectomies, ectropion uveae (magnified view of RE), iris transillumination (RE). Family 7 **(E)**: broad peripheral iridectomy, band keratopathy, iris stromal hypoplasia. Temporal peripheral corneal opacities in family 1 (II:1, bilateral), family 3 (II:3, RE), and family 7 (II:1, RE) were a suspected consequence of surgery.

Table 1. *CPAMD8* Variants Associated with Anterior Segment Dysgenesis and Glaucoma

Family	gDNA	cDNA	Exon	Protein	gnomAD AC (AF)	CADD	PP2	SIFT
1	chr19:g.17038927G>A	c.3403C>T	25	p.(Arg1135Ter)	10/276872 (0.00003612)	38		
	chr19:g.17036131G>A	c.3563C>T	26	p.(Pro1188Leu)	4/246198 (0.00001625)	25.9	1; D	0.031; D
2	chr19:g.17015130G>T	c.4298C>A	32	p.(Thr1433Asn)	5/276098 (0.00001811)	24.1	0.955; D	0.008; D
	chr19:g.17100491A>G	c.1498T>C	13	p.(Cys500Arg)		25.7	0.997; D	0.006; D
3	chr19:g.17015130G>T	c.4298C>A	32	p.(Thr1433Asn)	5/276098 (0.00001811)	24.1	0.955; D	0.008; D
	chr19:g.17100523A>G	c.1466T>C	13	p.(Leu489Pro)	1/245962 (0.000004066)	24.7	0.963; D	0.211; T
4	chr19:g.17081702dupC	c.2352dupC	18	p.(Arg785Glnfs*23)				
	chr19:g.17099980_17116595dup							
5	chr19:g.17081702dupC	c.2352dupC	18	p.(Arg785Glnfs*23)				
	chr19:g.17039805insGGA	c.3231_3232insGGA	24	p.(Ser1078delinsGlySer)				
6	chr19:g.17062979T>A	c.2449A>T	20	p.(Lys817Ter)		35		
7	chr19:g.17049229insG	c.2961dupG	23	p.(Tyr988LeufsTer9)	1/215022 (0.000004651)			

Position of each disease-associated variant with the human genome (hg19 reference), consensus transcript (NM_015692.5), and protein (NP_056507.3) described using HGVS nomenclature (version 15.11). Allele counts and allele frequencies of each variant in the gnomAD database (v2.1.1) are shown, as are Phred-scaled CADD (v1.4), PolyPhen-2 HVAR (PP2) and SIFT scores with predictions of deleteriousness. AC = allele count; AF = allele frequency; CADD = combined annotation dependent depletion; D = damaging/deleterious; T = tolerated.

Tolerant algorithms (Table 1). Alignment of vertebrate CPAMD8 protein sequences demonstrated strong conservation at the position of each of the missense variant residues (Fig 1E).

CPAMD8 is known to be expressed in the anterior segment of the developing human eye, with high expression in the developing human lens, iris, and cornea at 22 weeks' gestation.[8] We further assessed *CPAMD8* expression in an RNAseq dataset from ocular tissue of recently deceased adult donors and identified highest expression in the ciliary body and corneal epithelium with minimal expression in retina (Fig 1F), consistent with the expression pattern in the developing human eye.

Clinical data summarized across all 11 affected individuals revealed some key similarities to previously described cases of *CPAMD8*-associated ASD (Fig 2, Table 2, Table S1, available at www.aaojournal.org).[8] The majority of cases were noted to have 1 or more abnormalities of the iris (9/11), with a subset displaying stromal hypoplasia (6/11), iridodonesis (5/11), ectropion uveae (5/11), or corectopia (4/11) (Fig 2). There was a tendency toward high myopia, with a mean preoperative spherical equivalent of −8.56±9.37 D, although at least 1 individual was a +3.50 hyperope (family 3, II:3).

The majority of individuals (9/11, 81.8%) were diagnosed with glaucoma, all of whom (9/9) required incisional surgery to control IOP and most of whom (8/9, 88.9%) required multiple incisional procedures. The majority (6/11, 54.5%) of individuals were diagnosed with primary congenital glaucoma at birth, 1 with childhood glaucoma at 15 years of age, 2 with juvenile-onset open-angle glaucoma at 33 and 35 years of age, and 1 was receiving pharmacologic treatment for bilateral ocular hypertension at 53 years of age (family 6, II:2). Within our cohort, glaucoma penetrance was 54.5% (6/11) at 10 years of age and 63.6% (7/11) at 25 years of age. Across all reported *CPAMD8* cases, the cumulative glaucoma risk was 43.8% by 10 years of age and 50.0% by 25 years of age (95% confidence interval, 0−68 years) (Fig 3A).

Cataracts were present in 8 of 11 individuals (72.7%). The presence of buphthalmos in the proband of family 2 (II:1) made this cataract surgery challenging, and the patient was left aphakic. Bilateral retinal detachment occurred in 3/11 individuals. Across all reported *CPAMD8* cases, the cumulative risk of cataract diagnosis or surgery was 50% at 33 years of age (95% confidence interval,

Table 2. Clinical Summary of Individuals with Biallelic *CPAMD8* Variants

Variable	Value
Female (%)	5/11 (45.5)
Best-corrected visual acuity (decimal)	0.42±0.32
Preoperative refraction (D)	−8.56±9.37
Cataract (%)	8/11 (72.7)
Age at cataract diagnosis or surgery (yrs)	35.75±12.28
Phacodonesis (%)	5/11 (45.5)
Ectopia lentis (%)	4/11 (36.4)
Iris stromal hypoplasia (%)	6/11 (54.5)
Ectropion uveae (%)	5/11 (45.4)
Iridodonesis (%)	5/11 (45.5)
Iris transillumination (%)	4/11 (36.4)
Corectopia (%)	3/11 (27.3)
Posterior embryotoxon (%)	1/11 (9.1)
Retinal detachment (%)	3/11 (27.3)
Age at first retinal detachment (yrs)	30±9.17
Glaucoma (%)	9/11 (81.8)
Age at glaucoma diagnosis (yrs)	9.22±14.89
Buphthalmos (%)	5/11 (45.5)
Haab striae (%)	2/11 (18.2)
Max IOP (mmHg)	36±10
Highest corneal diameter (mm)	14.3±1.7
Mean CCT (μm)	609±92
Worst VCDR	0.62±0.23
Worst mean deviation (dB)	−8.92±9.90

CCT = central corneal thickness; D = diopter; IOP = intraocular pressure; VCDR = vertical cup:disc ratio. Continuous variables are expressed as mean ± standard deviation and categoric variables as percentages.

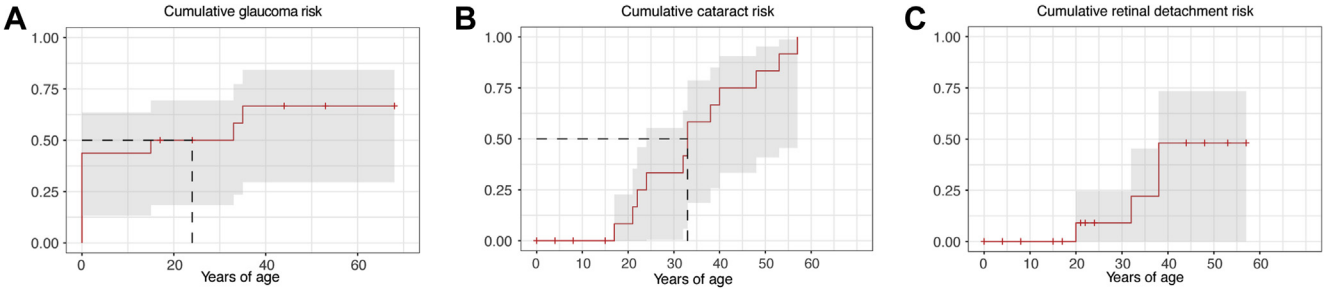

Figure 3. Age-associated prevalence of glaucoma, cataracts, or retinal detachment in individuals with bialleleic *CPAMD8* variants. Including the 11 cases described here, plus 5 previously reported cases.[3,8] **A,** Cumulative glaucoma risk, with a cumulative risk of 50% at 24 years of age **(dotted line)**. **B,** Cumulative cataract risk. Ages represent age at cataract diagnosis or age at cataract surgery (age at diagnosis used where both were known), with a cumulative risk of 50% at 33 years of age **(dotted line)**. **C,** Cumulative risk of retinal detachment in 1 or both eyes. Grey shading indicates 95% confidence intervals.

24−57 years) (Fig 3B), with a cumulative lifetime risk of retinal detachment in 1 or both eyes approaching 50%.

Discussion

We describe the largest cohort of individuals to date with biallelic variants in the *CPAMD8* gene and characterize its associated ocular phenotype. We provide evidence that this phenotype is broad, ranging from childhood and juvenile open-angle glaucoma with ASD to early-onset cataract and retinal detachments. Although consistently associated with abnormalities of the iris or lens, individuals with biallelic *CPAMD8* variants did not necessarily meet the definition of an existing disease entity. We note that in addition to ASD, biallelic *CPAMD8* variants can be associated with childhood and juvenile open-angle glaucoma, even in the absence of ectopia lentis. Within an Australian cohort of childhood glaucoma probands explained by any genetic diagnosis, biallelic *CPAMD8* variants accounted for at least 3.9% of individuals (5/129), second only to *CYP1B1,* which accounted for 16.3% in the same cohort. This was equivalent to the frequency associated with heterozygous loss-of-function variants in *TEK*[14] or *FOXC1*.[4] In our cohort of patients with juvenile-onset glaucoma diagnosed at 18 to 40 years of age, *CPAMD8* variants accounted for at least 1.4% (2/139) of probands, second only to *MYOC* (5/139, 3.6%), and at a frequency equivalent to *CYP1B1*.

It was also apparent that in several cases the clinical diagnosis was not clear initially, with several cases referred to as primary congenital glaucoma, despite the presence of anterior segment defects. This is not an uncommon occurrence in primary congenital glaucoma, for which diagnoses are often revised after examinations under anesthesia, resolution of corneal opacity, or in some cases in which a careful examination is prompted by a new molecular diagnosis.[4]

Not all *CPAMD8* variants were immediately apparent on exome sequencing, despite the presence of a known disease-associated frameshift variant and a strong phenotypic resemblance to other *CPAMD8*-associated cases. We found that in these cases, examination of copy number variants or less stringent filtering of exome sequencing data could reveal a second allele.[12] This has important implications for screening, where a heterozygous rare and predicted deleterious *CPAMD8* variant in a clinically compelling case should invite further molecular scrutiny of the second allele.

Ascertainment bias makes it difficult to accurately estimate glaucoma penetrance in *CPAMD8*-associated ASD. Within the limits of available patient data (16 total *CPAMD8* cases, including the 11 described), we estimated glaucoma penetrance in *CPAMD8*-related ASD to be 62.5% (10/16), which is similar to more reliable estimates in ARS.[1] Other causes of ASD, notably ARS caused by *FOXC1* or *PITX2* variants, have a well-defined association with glaucoma, with a glaucoma prevalence of 58.5% in a cohort of 53 cases.[2] The penetrance at age 10 years among individuals with *CPAMD8* (43.8%) was similar to previous estimates in individuals with *FOXC1* variants (42.9%).[2] Glaucoma is often difficult to treat in ARS,[1,15] and *CPAMD8*-associated ASD appears to be no exception, with all individuals in this report diagnosed with glaucoma requiring incisional surgery to control IOP and approximately 90% requiring multiple procedures. Family 1 (II:1) is a striking example; the proband, diagnosed with glaucoma within the first 2 weeks of life, required 5 IOP-lowering interventions in each eye within the first 4 years of life.

The *CPAMD8*-related ASD phenotype was associated with lens or iris anomalies in all affected individuals. Commonly associated ocular features included iris stromal hypoplasia (6/11), iris transillumination defects (4/11), corectopia (4/11), ectropion uveae (5/11), iridodonesis (5/11), and ectopia lentis (4/11). Polycoria, often seen in ARS associated with *FOXC1* and *PITX2* variation, was not reported in any reported *CPAMD8* cases, and posterior embryotoxon was reported in only 1 individual. Cataracts were present in 8 of 11 individuals. These phenotypes suggest lens instability and pupillary block as 1 potential underlying cause of *CPAMD8*-associated glaucoma, consistent with its predominant expression in the adult ciliary body. However, we observed glaucoma in at least 1 case diagnosed with buphthalmos at birth without lens instability (family 1, II:1), implying aqueous outflow dysfunction is also likely to be implicated. An array of anterior segment abnormalities also highlights the

challenges a surgeon could expect to encounter: for example, buphthalmos complicating cataract surgery and intraocular lens placement in family 2 (II:1). A requirement for multiple incisional procedures to control IOP (8/11), an increased rate of zonular instability (5/11), and bilateral retinal detachment (3/11) highlight further complexities in managing such patients.

CPAMD8 (complement component 3- and pregnancy zone protein-like alpha-2-macroglobulin domain-containing protein 8) is 1 of 8 members of the complement 3/α2-macroglobulin (C3/α2M) family reported in humans.[16] Other C3/α2M family members include the complement components C3, C4A, C4B, and C5; α2M; pregnancy zone protein; and CD109. C3, C4A, C4B, C5, and α2M proteins are all abundant in plasma, whereas CD109 is a GPI-anchored cell-surface molecule, and CPAMD8 is membrane associated. Although CPAMD8 was initially suspected to play a role in immunity, its physiologic function is still not known.[16] The conspicuous absence of a *CPAMD8* ortholog in rodent genomes makes this gene challenging to study in model organisms, although limited inference can be made from RNA expression studies. *CPAMD8* is consistently expressed in tissues of neural crest origin,[17] including the lens, iris, and cornea in utero,[8] and the ciliary body and corneal epithelium in adult eyes. This pattern is consistent with hypoplasia of the iris stroma in patients with *CPAMD8* variants, whereas neuroectoderm-derived pigmented epithelial cells develop normally. Other key drainage structures in the eye, including the trabecular meshwork and Schlemm's canal, are also derived from neural crest progenitors and may be hypoplastic or otherwise dysfunctional in the absence of CPAMD8. But unlike other ASDs defined by neural crest dysfunction,[18] *CPAMD8* deficiency does not appear to cause other neural crest−associated malformations involving dental, craniofacial, and aortic structures. With respect to the mechanism of high-pressure glaucoma, both outflow obstruction (through dysplasia or dysfunction of outflow structures) and lens instability (through ciliary zonule dysfunction) could be consistent with the observed *CPAMD8* expression patterns, although our analyses do not capture the full temporal and spatial variation of *CPAMD8* expression. In any case, the observation of 4 affected individuals with biallelic nonsense or frameshift variants suggests that loss of CPAMD8 function is responsible.

In conclusion, our findings reveal that biallelic *CPAMD8* variants are associated with a clinically heterogeneous phenotype, including frequent associations with autosomal recessive childhood glaucoma (3.9%) and juvenile open-angle glaucoma (1.4%). *CPAMD8* should be considered in the differential diagnosis of both childhood and juvenile open-angle glaucoma, particularly when associated with iris abnormalities, cataract, or retinal detachment. This phenotypic characterization has important implications for improved clinical care, including providing appropriate genetic testing and counseling, and more accurate prognostication of expected complications.

References

1. Shields MB. Axenfeld-Rieger syndrome: a theory of mechanism and distinctions from the iridocorneal endothelial syndrome. *Trans Am Ophthalmol Soc*. 1983;81:736−784.
2. Souzeau E, Siggs OM, Zhou T, et al. Glaucoma spectrum and age-related prevalence of individuals with FOXC1 and PITX2 variants. *Eur J Hum Genet*. 2017;25:839−847.
3. Alsaif HS, Khan AO, Patel N, et al. Congenital glaucoma and CYP1B1: an old story revisited. *Hum Genet*. 2019 Sep;138:1043−1049.
4. Siggs OM, Souzeau E, Pasutto F, et al. Prevalence of FOXC1 variants in individuals with a suspected diagnosis of primary congenital glaucoma. *JAMA Ophthalmol*. 2019;137:348−355.
5. Nishimura DY, Swiderski RE, Alward WL, et al. The forkhead transcription factor gene FKHL7 is responsible for glaucoma phenotypes which map to 6p25. *Nat Genet*. 1998;19:140−147.
6. Semina EV, Reiter R, Leysens NJ, et al. Cloning and characterization of a novel bicoid-related homeobox transcription factor gene, RIEG, involved in Rieger syndrome. *Nat Genet*. 1996;14:392−399.
7. Khan AO. Conditions that can be mistaken as early childhood glaucoma. *Ophthalmic Genet*. 2011;32:129−137.
8. Cheong S-S, Hentschel L, Davidson AE, et al. Mutations in CPAMD8 cause a unique form of autosomal-recessive anterior segment dysgenesis. *Am J Hum Genet*. 2016;99:1338−1352.
9. Hollmann AK, Dammann I, Wemheuer WM, et al. Morgagnian cataract resulting from a naturally occurring nonsense mutation elucidates a role of CPAMD8 in mammalian lens development. *PLoS One*. 2017;12:e0180665.
10. Souzeau E, Goldberg I, Healey PR, et al. Australian and New Zealand Registry of Advanced Glaucoma: methodology and recruitment. *Clin Exp Ophthalmol*. 2012;40:569−575.
11. Thau A, Lloyd M, Freedman S, et al. New classification system for pediatric glaucoma: implications for clinical care and a research registry. *Curr Opin Ophthalmol*. 2018;29:385−394.
12. Siggs OM, Javadiyan S, Sharma S, et al. Partial duplication of the CRYBB1-CRYBA4 locus is associated with autosomal dominant congenital cataract. *Eur J Hum Genet*. 2017;25:711−718.
13. Siggs OM, Souzeau E, Craig JE. Loss of ciliary zonule protein hydroxylation and lens stability as a predicted consequence of biallelic ASPH variation. *Ophthalmic Genet*. 2019:1−5.
14. Souma T, Tompson SW, Thomson BR, et al. Angiopoietin receptor TEK mutations underlie primary congenital glaucoma with variable expressivity. *J Clin Invest*. 2016;126:2575−2587.
15. Strungaru MH, Dinu I, Walter MA. Genotype-phenotype correlations in Axenfeld-Rieger malformation and glaucoma patients with FOXC1 and PITX2 mutations. *Invest Ophthalmol Vis Sci*. 2007;48:228−237.
16. Li Z-F, Wu X-H, Engvall E. Identification and characterization of CPAMD8, a novel member of the complement 3/alpha2-macroglobulin family with a C-terminal Kazal domain. *Genomics*. 2004;83:1083−1093.
17. Johnston MC, Noden DM, Hazelton RD, et al. Origins of avian ocular and periocular tissues. *Exp Eye Res*. 1979;29:27−43.
18. Kupfer C, Kaiser-Kupfer MI. Observations on the development of the anterior chamber angle with reference to the pathogenesis of congenital glaucomas. *Am J Ophthalmol*. 1979;88:424−426.

Footnotes and Financial Disclosures

Originally received: July 16, 2019.
Final revision: December 19, 2019.
Accepted: December 20, 2019.
Available online: ■■■. Manuscript no. D-19-00652.

[1] Department of Ophthalmology, Flinders University, Adelaide, Australia.

[2] SA Pathology, Adelaide, Australia.

[3] Centre for Eye Research Australia, Royal Victorian Eye and Ear Hospital, Melbourne, Australia.

[4] Department of Ophthalmology, University of Melbourne, Melbourne, Australia.

[5] Department of Ophthalmology, Royal Children's Hospital, Melbourne, Australia.

[6] Geelong Eye Centre, Geelong, Australia.

[7] Department of Ophthalmology, Children's Hospital at Westmead, Sydney, Australia.

[8] Discipline of Ophthalmology, University of Sydney, Sydney, Australia.

[9] Department of Ophthalmology, Macquarie University, Sydney, Australia.

[10] Menzies Institute for Medical Research, University of Tasmania, Hobart, Australia.

[11] Department of Paediatrics, University of Melbourne, Melbourne, Australia.

[12] Centre for Ophthalmology and Visual Science, University of Western Australia, Lions Eye Institute, Perth, Australia.

Financial Disclosure(s):
The author(s) have no proprietary or commercial interest in any materials discussed in this article.

Supported by the Channel 7 Children's Research Foundation, The Rebecca L Cooper Medical Research Foundation, and the Australian National Health & Medical Research Council (NHMRC) Centres of Research Excellence Grant APP1023911, Project Grant APP1107098).

K.P.B. and A.W.H.: Supported by an NHMRC Senior Research Fellowship.

J.E.C.: Supported by an NHMRC Practitioner Fellowship. The Centre for Eye Research Australia receives Operational Infrastructure Support from the Victorian Government. Funding organizations had no role in the design or conduct of this research.

HUMAN SUBJECTS: Human subjects were included in this study. Southern Adelaide Clinical Human Research Ethics Committee approved the study. All research adhered to the tenets of the Declaration of Helsinki All participants provided informed consent.

No animal subjects were used in this study.

Author Contributions:

Conception and design: Siggs, Souzeau, Craig

Data collection: Siggs, Souzeau, Taranath, Dubowsky, Chappell, Zhou, Javadiyan, Nicholl, Kearns, Staffieri, Narita, Smith, Pater, Hewitt, Ruddle, Elder, Mackey, Burdon, Craig

Analysis and interpretation: Siggs, Souzeau, Craig

Obtained funding: Siggs, Hewitt, Burdon, Craig

Overall responsibility: Siggs, Souzeau, Craig

Abbreviations and Acronyms:
ARS = Axenfeld-Rieger syndrome; **ASD** = anterior segment dysgenesis; **CADD** = combined annotation dependent depletion; **IOP** = intraocular pressure.

Correspondence:
Owen M. Siggs, MD, DPhil, Department of Ophthalmology, Flinders University, Bedford Park SA 5042, Australia, E-mail: owen.siggs@flinders.edu.au; and Emmanuelle Souzeau, PhD, Department of Ophthalmology, Flinders University, Bedford Park SA 5042, Australia. E-mail: emmanuelle.souzeau@flinders.edu.au.